Polymer Chemistry

A Dual Initiator Approach for Oxygen Tolerant RAFT Polymerization

Journal:	*Polymer Chemistry*
Manuscript ID	PY-ART-05-2022-000603.R1
Article Type:	Paper
Date Submitted by the Author:	24-Jul-2022
Complete List of Authors:	Taylor, Nicholas; University of North Carolina at Chapel Hill Department of Chemistry, Chemistry Reis, Marcus; University of North Carolina at Chapel Hill Department of Chemistry, Chemistry Varner, Travis; University of North Carolina at Chapel Hill Department of Chemistry, Chemistry Rapp, Johann; University of North Carolina at Chapel Hill Department of Chemistry, Chemistry Sarabia, Alexis; University of North Carolina at Chapel Hill Department of Chemistry, Chemistry Leibfarth, Frank; University of North Carolina at Chapel Hill Department of Chemistry, Chemistry

A Dual Initiator Approach for Oxygen Tolerant RAFT Polymerization

Nicholas G. Taylor, Marcus H. Reis, Travis P. Varner, Johann L. Rapp, Alexis Sarabia, Frank A. Leibfarth*

Department of Chemistry, University of North Carolina at Chapel Hill, Chapel Hill, NC 27599

Abstract:

Reversible-deactivation radical polymerizations are privileged approaches for the synthesis functional and hybrid materials. A bottleneck for conducting these processes is the need to maintain oxygen free conditions. Herein we report a broadly applicable approach to "polymerize through" oxygen using the synergistic combination of two radical initiators having different rates of homolysis. The *in situ* monitoring of the concentrations of oxygen and monomer simultaneously provided insight into the function of the two initiators and enabled the identification of conditions to effectively remove dissolved oxygen and control polymerization under open-to-air conditions. By understanding how the surface area to volume ratio of reaction vessels influence open-to-air polymerizations, well-defined polymers were produced using acrylate, styrenic, and methacrylate monomers, which each represent an expansion of scope for the "polymerizing through" oxygen approach. Demonstration of this method in tubular reactors using continuous flow chemistry provided a more complete structure–reactivity understanding of how reaction headspace influences PTO RAFT polymerizations.

Introduction

The radical polymerization of vinyl monomers represents nearly half of industrially produced polymers.[1] Radical polymerization is prized as a method of chain growth polymerization due to its tolerance to a wide variety of functional groups and ability to produce materials with a range of thermomechanical properties.[2,3] Such polymerizations are typically ran under an inert atmosphere due to the propensity for the propagating radical intermediate to react with triplet oxygen and form peroxy radicals or hydroperoxides.[4] This undesired reactivity can inhibit polymerization completely or result in a lowering of the number average molar mass (M_n), and an increase in the dispersity ($Đ$).[5] As such, the need to remove oxygen increases the production cost of material synthesis at an industrial scale.[6,7]

Reversible-deactivation radical polymerizations (RDRPs) are privileged approaches for the synthesis of functional and hybrid materials with a well-defined M_n and low $Đ$.[8,9] RDRP approaches typically exert control over chain-growth kinetics by maintaining a low concentration of propagating radicals in solution, making them particularly sensitive to the presence of dissolved oxygen. This has sparked the development of several innovative methods to make RDRP more oxygen tolerant.[5] For example, a variety of different approaches were developed that enabled oxygen tolerant atom transfer radical polymerizations (ATRP).[10,11,12,13,14] In contrast, less methods have been explored that enable oxygen tolerant reversible addition fragmentation chain transfer (RAFT) polymerizations. The most widely employed method for oxygen-tolerant RAFT polymerization leverages the reactivity of photocatalysts in their excited state for the conversion of triplet oxygen to singlet oxygen.[15] Other strategies to enable oxygen tolerant RAFT polymerizations rely on enzymatic degassing[16–24] or photoiniferter systems[25–32]. In all these examples, however, specific reaction conditions and/or additives are required to achieve oxygen tolerance. A more general and operationally simple method that enables

the synthesis of a wide variety of well-defined polymers under diverse reactions conditions remains an unsolved challenge.

"Polymerizing through" oxygen (PTO) is a nascent approach to achieve oxygen tolerant RAFT polymerizations.[33] PTO relies on the generation of a high flux of radicals at the beginning of a polymerization to rapidly convert oxygen into peroxy radicals or hydroperoxides that are inefficient at initiation and have high thermal stability.[6] Subsequent radical generation initiates polymerization. Early observations of PTO indicated that oxygen did not significantly retard RAFT polymerizations when using high initiator concentrations.[34] Perrier and coworkers intentionally exploited this concept for the preparation of multiblock copolymers by demonstrating that the generation of a high flux of radicals at an elevated temperature in water can simultaneously remove oxygen and provide high-fidelity polymerization of acrylamide monomers (**Figure 1A**).[35–37] The selection of an azo initiator that decomposes quickly at the reaction temperature (half-life of 77 seconds at 100 °C) and a monomer class with a rapid propagation rate enabled this approach by minimizing inhibition periods typically observed during RAFT polymerization in the presence of oxygen.[38] Despite the success of this PTO strategy for high throughput synthesis, this approach has been restricted to the polymerization of acrylamide monomers in water.[39,40] Previous work from our lab empirically discovered that oxygen tolerant RAFT polymerizations of acrylic comonomers in organic solvents was possible using two azo initiators with different decomposition temperatures.[41] We hypothesized that a two-stage decomposition profile originating from the initiators could provide a more broadly applicable approach to polymerizing through oxygen, where the high concentration of radicals early in the polymerization would deplete dissolved oxygen, and the low and consistent radical generation thereafter would provide initiation of RAFT polymerization.

Herein, we describe a dual initiator approach to PTO that enables temporal control over radical flux during a polymerization, where one initiator decomposes rapidly to consume dissolved oxygen and a second initiator generates radicals slowly to initiate controlled RAFT polymerizations (**Figure 1B**). The

synergistic combination of radical initiators provides controlled polymerization under open-to-air conditions of acrylates, styrenics, and methacrylates, which each represent new monomers classes for use in a PTO RAFT strategy. The ability to simultaneously monitor the kinetics of monomer and oxygen consumption *in situ* allowed us to identify initiator concentrations that lead to controlled polymerizations. Translation of these conditions into a flow reactor demonstrated the feasibility of performing controlled, oxygen tolerant RAFT polymerizations in a rapid, continuous system. This operationally simple approach to PTO RAFT polymerizations will be potentially valuable for both large scale process chemistry and the high throughput synthesis of complex materials on small scale.[42–46]

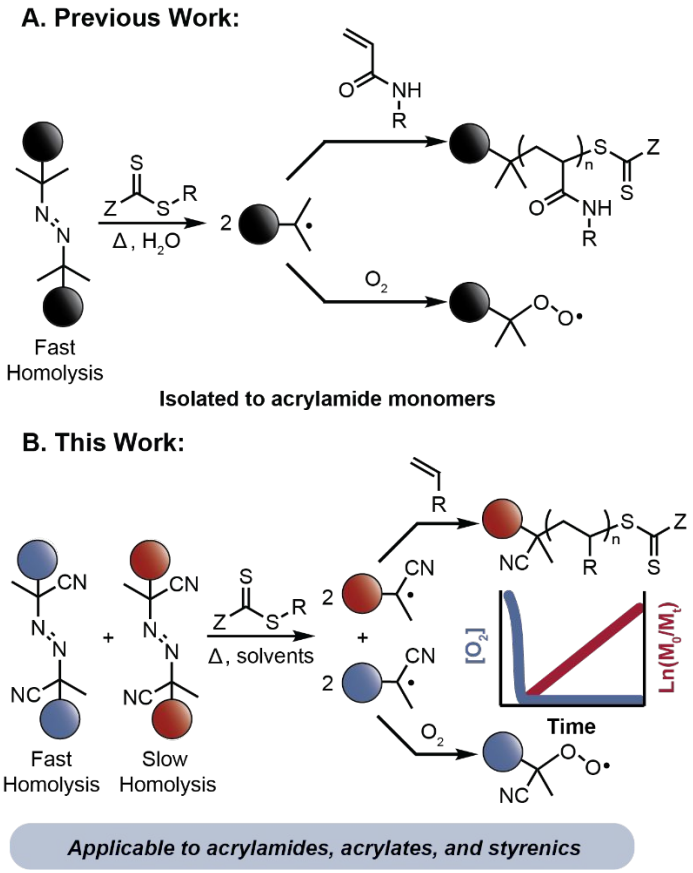

Figure 1. Previous work (**A**) uses a low decomposition-temperature azo initiator to enable oxygen-tolerant polymerizations of acrylamide monomers in aqueous solution. This work (**B**) uses two azo

initiators with different rates of homolysis to expand the scope of oxygen-tolerant RAFT polymerization to a diverse range of monomers and reaction conditions.

Results and Discussion

Optimization of initiator ratios for oxygen-tolerant polymerizations

In order to expand the dual initiator approach[41] to work for a variety of monomers with different reactivity profiles, a more quantitative understanding of reaction rates governing oxygen depletion and monomer polymerization was required. Azobisisobutyronitrile (AIBN) and 2,2'-Azobis(4-methoxy-2.4-dimethyl valeronitrile) (V-70) where chosen as azo initiators with significantly different decomposition profiles, demonstrating 10-hour half-life decomposition temperatures of 65 ºC and 30 ºC, respectively. These initiators are also both soluble in organic solvents, which we hypothesized would enhance the scope of PTO RAFT beyond reactions conducted in water. To aid in understanding the time evolution of radical concentration in a reaction that includes both AIBN and V-70, a simulation was performed that estimated the radical concentration at 80 °C in a reaction containing either 2 mM V-70, 6 mM AIBN, or a combination of the two (**Figure 2**). The initiator concentrations were chosen based on our previous empirical observations, and the homolysis rate constants were estimated assuming Arrhenius behavior. The simulation, which does not consider the effect of radical termination, demonstrated that V-70 homolysis creates a high flux of radicals within the first 5 minutes, whereas AIBN decomposes more slowly. The combination of the two initiators showed an initial high flux of radicals, followed by a steady flux of radicals after approximately 8 minutes.

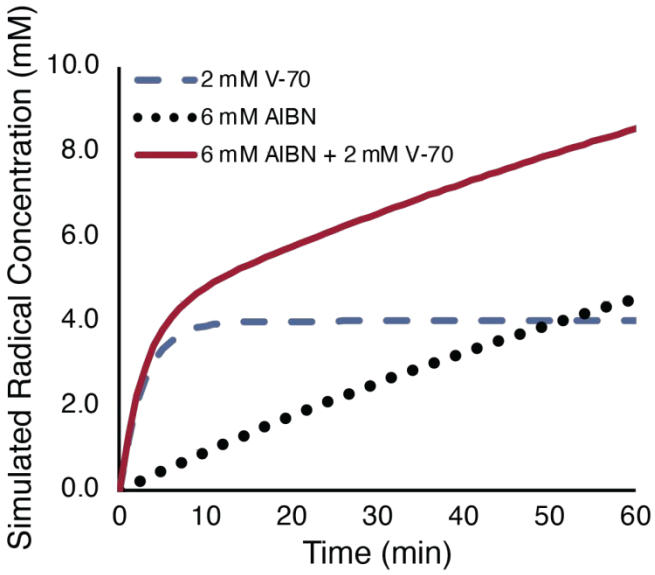

Figure 2. Simulated radical concentrations with respect to time in polymerizations containing 2 mM V-70 (blue dashed line), 6 mM AIBN (black dotted line), and a combination of 6 mM AIBN and 2 mM V-70 (red solid line) at 80 °C. The rate constants for each initiator were estimated using the activation energies and frequency factors supplied by Wako chemical company. These simulations do not include any contributions from radical termination events.

The RAFT polymerization of *n*-butyl acrylate was used for method development. Acrylic monomers had not previously been optimized for PTO RAFT approaches; therefore, this experiment represents an increase in the scope of this nascent approach for controlled polymerizations. The real time, simultaneous monitoring of both solution oxygen concentration ($[O_2]$) and monomer conversion was particularly enabling. Polymerizations were conducted at 80 °C in a closed triple neck flask equipped with two probes—one enabling the *in situ* quantification of $[O_2]$ and the other helping to determine reaction kinetics using *in situ* infrared spectroscopy by monitoring the disappearance of the *n*-butyl acrylate alkene stretch at 1650 cm^{-1}. Dioxane was initially chosen as solvent for its high oxygen solubility compared to other organic solvents.[47] We hypothesized that optimizing reaction conditions with dioxane

would enable the generalization of the approach to other organic solvents. Initiating the polymerization with 6 mM V-70 as the sole initiator demonstrated oxygen removal after 1.5 minutes and subsequent non-linear kinetics with a plateau in monomer conversion after 15 minutes of polymerization (61 % *n*-butyl acrylate conversion, 96% of V-70 decomposition) (**Figure S1**). In contrast, a separate experiment with 6 mM AIBN as the sole initiator resulted in a 31-minute inhibition period (**Figure S2 & S3**), which underscored the importance of using an initiator that undergoes quick decomposition for reproducible PTO RAFT polymerizations.

As indicated by the simulation, a V-70 concentration of 2 mM rapidly depleted dissolved oxygen in solution experimentally and polymerized *n*-butyl acrylate to high conversion in a non-degassed reaction vial (**Figure S4**). An inflection point in pseudo first-order behavior was apparent that resulted in a kinetic profile with two distinct linear regimes. The first and steepest regime was observed during the first 10 minutes of polymerization, at which time an estimated 90% of the V-70 and 8% of the AIBN had homolyzed. Polymerization during this initial period, therefore, is largely attributed to polymerization initiated by V-70 after oxygen consumption. A similar but less pronounced two-stage polymerization was observed when decreasing the V-70 concentration to 500 μM (**Figure 3A**). Reducing the V-70 concentration further to 300 μM was sufficient for the complete removal of dissolved oxygen after 4.5 minutes (**Figure 3B**) and resulted in a polymerization that demonstrated pseudo first-order kinetic behavior. We hypothesize that this concentration of V-70 was sufficient to consume dissolved oxygen, which enabled the radicals generated by the decomposition of AIBN to be predominately responsible for the observed polymerization kinetics. Presumably, radicals formed from AIBN and V-70 homolysis may also contribute to oxygen consumption or monomer initiation, respectively. Decreasing V-70 concentration further (100 μM) led to a significant inhibition period of 21 minutes before observable monomer conversion, likely due to incomplete removal of dissolved oxygen by the V-70 initiator (**Figure 3C**).

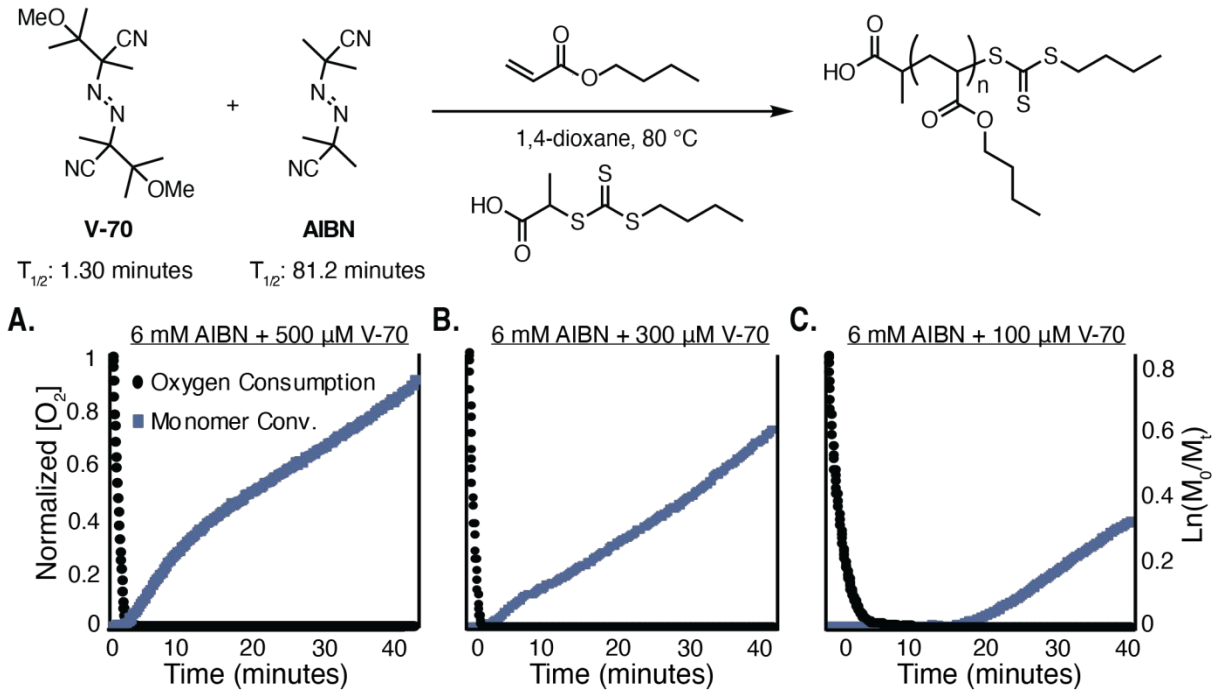

Figure 3. Oxygen consumption and monomer conversion of *n*-butyl acrylate RAFT polymerizations conducted with 6 mM of AIBN and 500 µM V-70 (**A**), 300 µM V-70 (**B**), and 100 µM V-70 (**C**). Conditions: [*n*-butyl acrylate] = 2 M, [CTA] = 10 mM in dioxane at 80 ºC. Radical initiator half-lives estimated from the Arrhenius equation at 80 ºC.

Identification of experimental parameters to enable open-to-air polymerizations

With initiator concentrations optimized, the diffusion of oxygen from the headspace into solution was investigated. Extensive work has shown that the diffusion of oxygen into solution is proportional to its interfacial surface area.[48–54] For example, oxygen-tolerant RAFT approaches relying on enzymatic degassing have reported the need to match enzymatic activity to the reaction vessel surface area so that the rate of oxygen consumption by the enzyme is faster than oxygen diffusion into solution.[17,22] PTO RAFT polymerizations could be viewed analogously, where the generation of new radical species over time could consume oxygen radicals at a faster rate than oxygen diffusion into solution. Accordingly, we

hypothesized that optimizing the polymerization surface-area-to-volume ratio (SA:V) would influence the rate of oxygen diffusion and enable controlled polymerizations in vessels open to air.

To test this hypothesis, a series of *n*-butyl acrylate polymerizations were left uncapped under ambient conditions in 2-dram vials with optimized initiator concentrations (6 mM AIBN and 300 μM V-70). This experimental design maintained a constant interfacial surface area while changing the total volume of each polymerization (**Figure 4**). The infinite headspace intrinsic to open-to-air polymerizations kept the rate of oxygen diffusion constant during these experiments, while also posing a significant challenge for achieving controlled radical polymerizations. In these experiments, we identified a trend where increasing SA:V (by decreasing solution volume) lowered monomer conversion and polymer molecular weight; the polymerization with the largest SA:V value produced no observable polymer. Conversely, a polymerization with a SA:V value of 0.60 produced low dispersity (< 1.30) materials that achieved their target molar mass (M_n). Capping the reaction vessels with an oxygen impermeable cap demonstrated less sensitivity to oxygen, with reaction outcomes that mirrored degassed polymerizations when SA:V < 1.2 (**Table S1**). This approach also displayed a high tolerance for stirring, only showing a deviation from expected monomer conversion with stirring speeds that effectively increased interfacial surface area through disrupting the solution-air interface (**Table S2**).

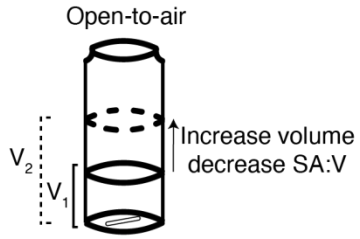

Liquid-air interfacial surface area (SA)
held constant by reactor diameter

SA:V (cm^{-1})[a]	Conv. (%)[b]	Theo. M_n (kg/mol)	Exp. M_n[c] (kg/mol)	$Đ$[c]
0.6	79	16.0	15.7	1.12
0.8	68	13.8	11.6	1.11
1.0	38	7.8	5.3	1.04
1.4	12	2.6	1.0	1.04
1.6	9	2.0	n.p.	n.p.

Figure 4. The effect of SA:V on control of thermal RAFT polymerizations. SA:V was systematically altered by changing the volume of the polymerization solution while keeping the surface area constant. Conditions: [*n*-butyl acrylate] = 2 M, [CTA] = 10 mM, [AIBN] = 6 mM, [V-70] = 300 μM, 80 °C, uncapped 2-dram vial, stirring for 30 minutes. [a]Interfacial surface area estimated by measuring the base of the vial. [b]Monomer conversion as determined from ^{1}H NMR using an internal standard. [c]Molecular weight and dispersity calculated using MALS on a THF GPC. n.p. indicates no observed polymerization.

The importance of the SA:V was further supported by using different sized vials, which intrinsically altered the interfacial surface area of each polymerization. Reactions with a SA:V value of 0.60 produced similar polymers regardless of reactor size (**Table S3**), demonstrating the generality of these experimental conditions for oxygen tolerant RAFT polymerizations. Polymers were even synthesized under open-to-air conditions on a larger scale (12 mL, SA:V = 0.60), which demonstrated the feasibility of scaling up open-to-air RAFT polymerizations (**Figure S5**).

The kinetics of open-to-air *n*-butyl acrylate polymerizations were evaluated at a SA:V value of 0.60. A plot of experimental M_n against monomer conversion with polymerizations targeting a degree of polymerization (DP) of 200 shows a close agreement with target molar masses (**Figure S6, Figure S7**). The linear increase in molar mass corroborated the initial pseudo first-order kinetic data observed from monomer conversion, further confirming the control over these thermally initiated RAFT polymerizations. Higher molecular weights were achieved by targeting a DP of 400. The molar masses of the resulting polymers deviate from their expected values at high conversion (>60%) and demonstrated dispersities approaching 1.30 (**Figure S8**). An experiment excluding the RAFT CTA demonstrated that the kinetic chain length under these conditions is <100 kg/mol, which indicates an inherent limitation of achieving high molar mass under these experimental conditions (**Table S4**).

Expanding the monomer scope

Expanding the scope of PTO RAFT to acrylates motivated the exploration of this method for other monomers.[41] We hypothesized that the use of this dual initiator platform would enable controlled polymerization using different RAFT chain transfer agents in a variety of solvents, thus demonstrating the versatility of this method compared to previous strategies run exclusively in DMSO or water.[17–24,55–63] First, polymerizations of *tert*-butyl acrylate and 2-ethylhexyl acrylate were investigated open-to-air under identical conditions to *n*-butyl acrylate polymerizations and displayed similar control, producing poly(acrylates) near theoretical M_n with low dispersities (**Figure 5**, **Figure S9**).

The reaction conditions were separately optimized for the other monomer classes (**Figure S10A-E**). For instance, when using dimethylformamide (DMF) as a solvent, this approach was successful in polymerizing the acrylamide monomers *N*-acryloylmorpholine and *N*-(isobutoxymethyl)acrylamide with excellent control (**Figure 5**, **Figure S11**). Increasing monomer concentration enabled access to higher molecular weight poly(*N*-acryloylmorpholine) (DP = 200, M_n = 20.5 kg/mol, Đ = 1.08) (**Figure S12**).

The effectiveness of a two azo initiator approach was further applied to control the RAFT polymerization of challenging monomers that demonstrate a slower rate of propagation. For the polymerization of styrenics, higher monomer concentrations (3 M), higher temperatures (100 ºC), and longer reaction times (2 hours) were required to expedite the synthesis of high molecular weight polymers (**Figure 5**, **Figure S13**). Optimization revealed that switching AIBN to an azo initiator that decomposes at a slower rate, such as 1,1'-Azobis(cyclohexanecarbonitrile) (ABCN), was essential for keeping radical flux to a minimum at higher operating temperatures.[64] The resulting polystyrene materials closely matched the target molar mass and maintained low dispersities ($Đ < 1.2$). Copolymerization of styrene with oxygen to form copolymer peroxides has been reported;[65–70] however, no peroxide was observed using ^{1}H NMR and ^{13}C NMR analyses under these conditions (**Figures S14-S15**).[66] Styrene polymerizations performed with no exogenous initiators demonstrated the minor role of styrene self-initiation, showing low monomer conversion (9 %) and negligible molar mass (M_n = 1500 g/mol) (**Table S5**). Polymerization of *tert*-butyl styrene using the PTO RAFT strategy demonstrated behavior similar to

the analogous degassed polymerization (**Figure S10B**) and considerably improved from the open-to-air polymerizing using a single initiator (**Table S7**).

Methacrylate polymerizations were more sensitive to oxygen, and required high temperatures, short reaction times, and capping of the reaction vessel to achieve controlled PTO RAFT polymerization. The polymers produced from this approach achieved molar masses near their targeted value with dispersities below 1.30 (**Figure 5**, **Figure S16**). The dual initiating system is considerably better than either of the two initiators individually, which produced polymer with low molar masses and higher dispersities (**Table S5** and **S6**). Expanding the exploration to poly(isobornyl methacrylate) also demonstrated molar masses and dispersity values similar to the analogous degassed polymerization (**Figure S10E**).

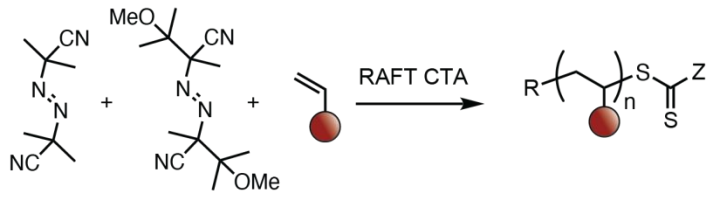

AIBN V-70

Monomer	Conv. [a] (%)	Theo. M_n (kg/mol)	Exp. $M_{n,MALS}$ (kg/mol)	Dispersity
1[b]	78	18.0	15.6	1.08
2[b]	64	14.9	11.0	1.05
3[b]	78	25.7	23.3	1.15
4[c]	75	10.0	10.1	1.09
5[c]	67	10.1	11.8	1.13
6[d]	35	11.0	11.9	1.12
7[d]	66	19.8	39.3	1.40
8[e]	49	11.4	13.3	1.26
9[e]	55	15.6	24.4	1.31

Monomers:

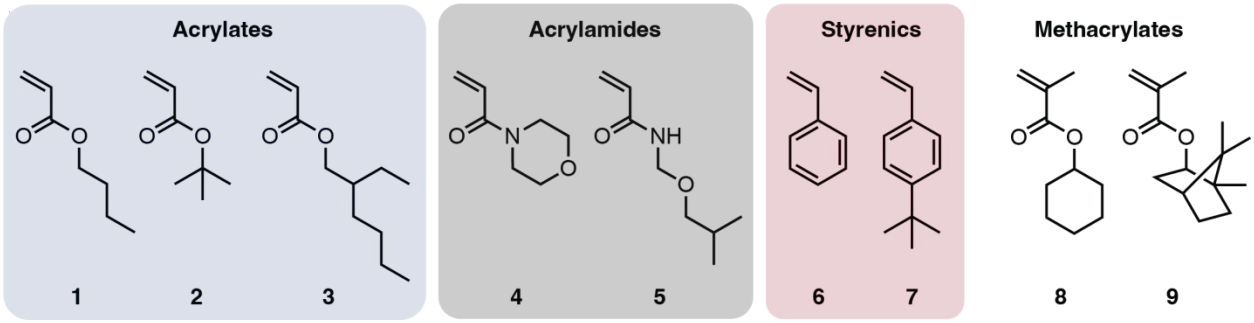

Figure 5. PTO RAFT polymerizations of different monomer classes under batch conditions. Conditions: [AIBN] = 6 mM, [V-70] = 300 uM, uncapped 2-dram vial, 300 rpm stirring, SA:V value of 0.60. All polymer molecular weights were calculated using multi-angle light scattering. [a]Conversion calculated from ^{1}H NMR relative to an internal standard. [b]2-(butylthiocarbonothioylthio) propanoic acid (BTTCP) used as the CTA in a monomer:CTA molar ratio of 200:1 in dioxane at 80 ºC and ran for 30 minutes. [c]Cyanomethyl dodecyl trithiocarbonate (CMDT) used as the CTA in a monomer:CTA molar ratio of 100:1 in DMF at 80 ºC and ran for 15 minutes. [d]Dibenzyl trithiocarbonate (DBTTC) used as the CTA in a monomer:CTA molar ratio of 300:1 in dichlorobenzene with 6 mM ABCN used in place of AIBN at 100 ºC and ran for 2 hours. [e]2-cyano-2-propyl benzodithioate (CPDB) used as the CTA in a monomer:CTA molar ratio of 200:1 in toluene and reaction vessel capped at 100 ºC and ran for 20 minutes.

The chain-end fidelity of different polymer classes made from this oxygen-tolerant approach was explored through chain-extension experiments (**Figure 6**). Polymerizations of *n*-butyl acrylate, *N*-acryoylmorpholine, and *tert*-butylstyrene were performed under their optimized, open-to-air reaction to target a DP of approximately 20. The resulting macro-RAFT CTAs of *n*-butyl acrylate (M_n = 1.7 kg/mol, $Đ$ = 1.06), *N*-acryloylmorpholine (2.7 kg/mol, $Đ$ = 1.11), and *tert*-butylstyrene (M_n = 1.7 kg/mol, $Đ$ = 1.07) were then subjected to open-to-air reaction conditions targeting higher DPs. The resulting polymerizations produced higher molecular weight acrylate (DP = 200, M_n =18.3 kg/mol, $Đ$ = 1.12), acrylamide (DP = 200, M_n = 31.8 kg/mol, $Đ$ = 1.16), and styrenic (DP = 300, M_n = 46.3 kg/mol, $Đ$ = 1.33) materials. In each case, a monomodal GPC chromatogram was observed with complete extension of the macro-RAFT CTA, which indicated a high degree of chain-end fidelity resulting from this dual initiator approach. Furthermore, the apparent low molecular weight tailing following chain extension was consistent with the tailing observed in degassed polymerizations (**Figure S17**).

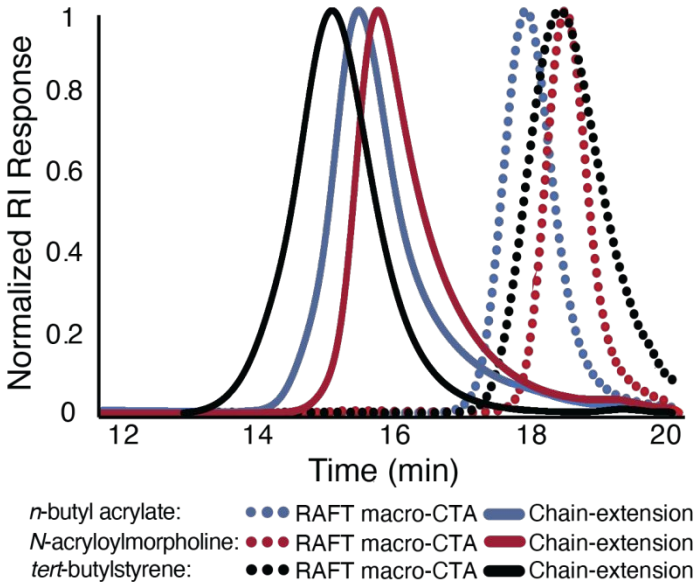

Figure 6. GPC chromatograms of polymers made from chain-extension experiments. Macro-RAFT CTAs and chain-extended polymers made from *n*-butyl acrylate (blue), *N*-acryloylmorpholine (red), and *tert*-butylstyrene (black) were synthesized under optimized, open-to-air reaction conditions and purified for analysis.

In a set of control experiments, the two initiators were used individually to assess their performance with a diverse range of monomers in open-to-air polymerizations at a SA:V of 0.60. The use of only V-70 at concentrations of either 1 mM or 6 mM resulted in a decrease in conversion and M_n for all substrates (**Table S5**). Notably, styrene polymerizations initiated with V-70 only achieved one-fourth of the molecular weight achieved by the dual initiator approach, despite having very similar monomer conversions. Similarly, methacrylate polymerizations required higher concentrations of V-70 to achieve polymerization, with 6 mM V-70 only achieving 25 % conversion and low molecular weight materials. The use of an AIBN concentration of 6 mM as the sole initiator displayed similar kinetics and polymer molecular weights as the dual initiating approach for styrene and *N*-acryloyl morpholine, but for *n*-butyl acrylate and cyclohexyl-methacrylate exhibited an approximately 20-30% lower monomer conversion and molar mass (**Table S6**).

Translation of the dual initiator approach into continuous flow

Continuous-flow chemistry is a platform technology that has several advantages over batch processes, such as improved heat transfer, mixing, and the potential for scale-up and automation.[71] Upon appropriate selection of oxygen-impermeable tubing, polymerizations run in flow provide a SA:V value approaching zero. Therefore, studying PTO RAFT polymerizations in tubular reactors would extend our understanding of how SA:V influences reaction outcome under a broader set of experimental conditions. A series of experiments were performed to directly compare batch *n*-butyl acrylate polymerizations to analogous polymerizations performed in a continuous flow system (**Figure S18).** A method developed by

Moore and coworkers was used to obtain continuous flow polymerization kinetics.[72] A polymerization initiated using the dual initiator conditions (6 mM AIBN and 300 μM V-70) under continuous-flow conditions produced well-defined materials (M_n = 12 kg/mol, $Đ$ = 1.10), with an inhibition period of 2 minutes and 50 seconds (**Figure 7A)**. This inhibition period was similar to what was observed under batch conditions (SA:V = 0.60). Additionally, the observed pseudo-first order kinetics indicated the successful translation of controlled PTO RAFT polymerizations into continuous flow. A faster rate was observed than the analogous batch reaction, which is likely attributed to the lack of headspace, improved heat transfer and enhanced mixing intrinsic to continuous flow chemistry. Polymerizations initiated with only 6 mM AIBN demonstrated a longer inhibition period of 3 minutes and 30 seconds, producing a material with similar properties (M_n = 14.9 kg/mol, $Đ$ = 1.08) at a similar rate to the dual initiator approach (**Figure 7B**). Lastly, polymerizations initiated with 6 mM V-70 exhibited the shortest inhibition time of 2 minutes but demonstrated a kinetic profile that deviated from first order at moderate conversions (**Figure 7C**).

The success of the PTO RAFT polymerization of *n*-butyl acrylate in a continuous flow reactor prompted the exploration of the other monomer classes. Using the same optimized polymerization conditions previously described in Figure 5, polymerizations of acrylates, acrylamides, styrenics, and methacrylates were conducted in continuous flow. Here, all monomers were polymerized effectively with a single initiator approach (AIBN or ABCN) and the dual initiator approach to produce polymers with similar molar mass and dispersity (**Figure 7D**). We attribute the success of the single and dual initiator approaches to the diminished oxygen diffusion present in flow due to a lack of headspace, resulting in shorter inhibition periods for AIBN- or ABCN-initiated polymerizations. In contrast, identical polymerizations run with 6 mM V-70 had slower kinetics with every monomer, despite having a large initial flux of radicals (**Table S7**).

The polymerization results in continuous flow illuminated the critical role that reaction head space plays in PTO RAFT polymerizations. We conclude that the dual initiator approach is useful for

open-to-air polymerizations with SA:V < 0.60. In contrast, the use of sufficient quantities of a single, high homoylsis temperature initiator is sufficient for continuous flow polymerizations where SA:V is effectively zero, assuming the application can tolerate a slightly longer incubation period. These results in flow reactors provide a more complete understanding of the structure–reactive relationships in PTO RAFT polymerizations.

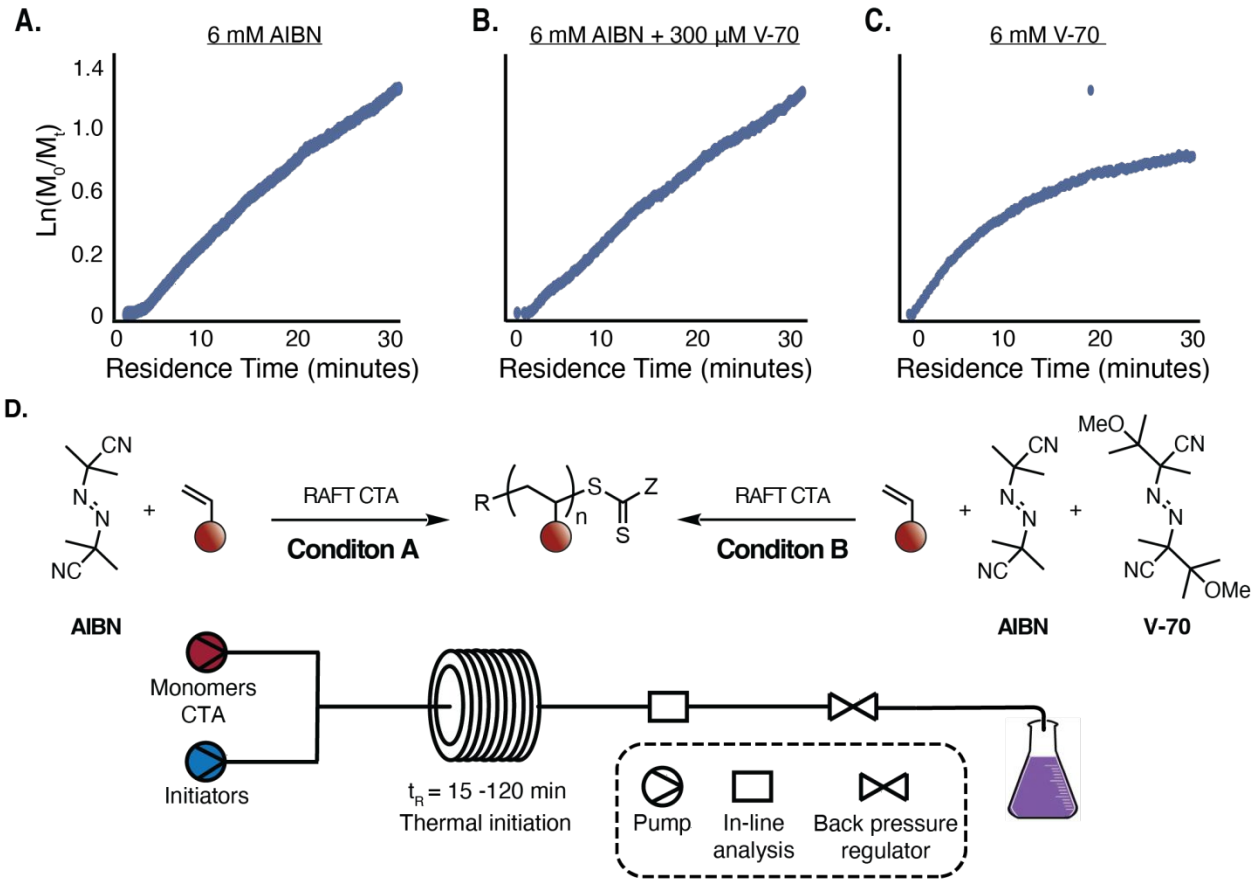

Monomer	Conv (%). [a]		Theo. M_n (kg/mol)		Exp. $M_{n,MALS}$ (kg/mol)		Dispersity	
	A	B	A	B	A	B	A	B
1[b]	67	75	15.5	17.3	14.9	12.0	1.08	1.10
2[b]	74	74	17.1	17.1	17.5	16.5	1.11	1.06
3[b]	74	76	24.4	25.1	21.4	17.4	1.29	1.23
4[c]	85	82	11.5	11.1	12.3	12.0	1.08	1.06
5[c]	52	59	7.9	8.9	12.0	10.2	1.05	1.05
6[d]	42	34	12.7	10.3	10.8	10.0	1.31	1.24
7[d]	59	61	18.2	18.8	28.6	27.0	1.42	1.40
8[e]	52	53	11.8	12.1	9.4	7.5	1.29	1.21
9[e]	50	48	15.0	14.4	17.5	16.0	1.27	1.23

Figure 7. Kinetics of *n*-butyl acrylate PTO RAFT polymerizations ran with 6 mM AIBN (**A**), 6 mM AIBN and 300 µM V-70 (**B**), and 6 mM V-70 (**C**). PTO RAFT polymerizations conducted in continuous flow with either 6 mM AIBN (Condition A) or 300 µM V-70 and 6 mM AIBN (Condition B) (**D**). All polymer molecular weights were calculated using multi-angle light scattering. Conditions: [AIBN] = 6 mM, [V-70] = 300 uM (Condition A) or solely [AIBN] = 6 mM (Condition B). [a]Conversion calculated

from ^{1}H NMR relative to an internal standard. [b]2-(butylthiocarbonothioylthio)propanoic acid (BTTCP) used as the CTA in a monomer:CTA molar ratio of 200:1 in dioxane at 80 ºC and ran for 30 minutes. [c]Cyanomethyl dodecyl trithiocarbonate (CMDT) used as the CTA in a monomer:CTA molar ratio of 100:1 in DMF at 80 ºC and ran for 15 minutes. [d]Dibenzyl trithiocarbonate (DBTTC) used as the CTA in a monomer:CTA molar ratio of 300:1 in dichlorobenzene with 6 mM ABCN used in place of AIBN at 100 ºC and ran for 2 hours. [e]2-cyano-2-propyl benzodithioate (CPDB) used as the CTA in a monomer:CTA molar ratio of 200:1 in toluene at 100 ºC and ran for 20 minutes.

Conclusions

Kinetic and experimental studies demonstrated that a synergistic combination of two thermally latent radical initiators facilitated the temporal control of radical flux during a polymerization. This dual initiator approach to PTO RAFT enabled the polymerization of a variety of monomers in open-to-air conditions that achieve values of M_n and $Đ$ analogous to polymerization performed under an inert atmosphere. SA:V ratio is an important parameter to consider to achieve controlled RAFT polymerizations conducted under open-to-air conditions, with a SA:V ratio <0.60 producing well defined polymers. Further, continuous flow polymerizations, where reaction headspace is not a concern, proved to be an operationally simple, scalable, and efficient technology to conduct PTO RAFT polymerization without the need to degas reagent solutions. We envision that the dual initiator strategy for PTO RAFT polymerizations will prove to be a broadly applicable and versatile approach for controlled polymerizations run at small and large scale.

ASSOCIATED CONTENT

Supporting Information. This material is available free of charge via the Internet at http://pubs.acs.org

AUTHOR INFORMATION

Corresponding Author

* Frank A. Leibfarth − Department of Chemistry, University of North Carolina at Chapel Hill, Chapel Hill, North Carolina 27599, United States; orcid.org/0000-0001-7737-0331; Email: FrankL@email.unc.edu

ACKNOWLEDGEMENTS

F. A. L. acknowledges support from the National Institute of General Medical Sciences under award no. R35-GM142666. The UNC Department of Chemistry's NMR Core Laboratory provided expertise and instrumentation that enabled this study with support from National Science Foundation (CHE-1828183 and CHE-0922858).

References

(1) Nesvadba, P. Radical Polymerization in Industry. In *Encyclopedia of Radicals in Chemistry, Biology and Materials*; John Wiley & Sons, Ltd: Chichester, UK, 2012.

(2) Hutchinson, R. A.; Penlidis, A. Free-Radical Polymerization: Homogeneous Systems. In *Polymer Reaction Engineering*; Blackwell Publishing Ltd: Oxford, UK; pp 118–178.

(3) Moad, G.; Solomon, D. *The Chemistry of Radical Polymerization*; Elsevier, 2005.

(4) Bhanu, V. A.; Kishore, K. Role of Oxygen in Polymerization Reactions. *Chem. Rev.* **1991**, *91* (2), 99–117.

(5) Yeow, J.; Chapman, R.; Gormley, A. J.; Boyer, C. Up in the Air: Oxygen Tolerance in Controlled/Living Radical Polymerisation. *Chem. Soc. Rev.* **2018**, *47* (12), 4357–4387.

(6) Ligon, S. C.; Husár, B.; Wutzel, H.; Holman, R.; Liska, R. Strategies to Reduce Oxygen Inhibition in Photoinduced Polymerization. *Chem. Rev.* **2014**, *114* (1), 557–589.

(7) Wight, F. R. Oxygen Inhibition of Acrylic Photopolymerization. *J. Polym. Sci. Polym. Lett. Ed.* **1978**, *16* (3), 121–127.

(8) Hawker, C. J.; Wooley, K. L. The Convergence of Synthetic Organic and Polymer Chemistries. *Science (80-.).* **2005**, *309* (5738), 1200–1205.

(9) Corrigan, N.; Jung, K.; Moad, G.; Hawker, C. J.; Matyjaszewski, K.; Boyer, C. Reversible-

Deactivation Radical Polymerization (Controlled/Living Radical Polymerization): From Discovery to Materials Design and Applications. *Prog. Polym. Sci.* **2020**, *111*, 101311.

(10) Matyjaszewski, K.; Dong, H.; Jakubowski, W.; Pietrasik, J.; Kusumo, A. Grafting from Surfaces for "Everyone": ARGET ATRP in the Presence of Air. *Langmuir* **2007**, *23* (8), 4528–4531.

(11) Jakubowski, W.; Min, K.; Matyjaszewski, K. Activators Regenerated by Electron Transfer for Atom Transfer Radical Polymerization of Styrene. *Macromolecules* **2006**, *39* (1), 39–45.

(12) Sun, Y.; Lathwal, S.; Wang, Y.; Fu, L.; Olszewski, M.; Fantin, M.; Enciso, A. E.; Szczepaniak, G.; Das, S.; Matyjaszewski, K. Preparation of Well-Defined Polymers and DNA–Polymer Bioconjugates via Small-Volume EATRP in the Presence of Air. *ACS Macro Lett.* **2019**, *8* (5), 603–609.

(13) Magenau, A. J. D.; Strandwitz, N. C.; Gennaro, A.; Matyjaszewski, K. Electrochemically Mediated Atom Transfer Radical Polymerization. *Science (80-.).* **2011**, *332* (6025), 81–84.

(14) Szczepaniak, G.; Fu, L.; Jafari, H.; Kapil, K.; Matyjaszewski, K. Making ATRP More Practical: Oxygen Tolerance. *Acc. Chem. Res.* **2021**, *54* (7), 1779–1790.

(15) Phommalysack-Lovan, J.; Chu, Y.; Boyer, C.; Xu, J. PET-RAFT Polymerisation: Towards Green and Precision Polymer Manufacturing. *Chem. Commun.* **2018**, *54* (50), 6591–6606.

(16) Yuan, B.; Huang, T.; Wang, X.; Ding, Y.; Jiang, L.; Zhang, Y.; Tang, J. Oxygen-Tolerant RAFT Polymerization Catalyzed by a Recyclable Biomimetic Mineralization Enhanced Biological Cascade System. *Macromol. Rapid Commun.* **2022**, *43* (1), 2100559.

(17) Schneiderman, D. K.; Ting, J. M.; Purchel, A. A.; Miranda, R.; Tirrell, M. V.; Reineke, T. M.; Rowan, S. J. Open-to-Air RAFT Polymerization in Complex Solvents: From Whisky to Fermentation Broth. *ACS Macro Lett.* **2018**, *7* (4), 406–411.

(18) Liu, Z.; Lv, Y.; An, Z. Enzymatic Cascade Catalysis for the Synthesis of Multiblock and Ultrahigh-Molecular-Weight Polymers with Oxygen Tolerance. *Angew. Chemie* **2017**, *129* (44), 14040–14044.

(19) Lv, Y.; Liu, Z.; Zhu, A.; An, Z. Glucose Oxidase Deoxygenation−redox Initiation for RAFT Polymerization in Air. *J. Polym. Sci. Part A Polym. Chem.* **2017**, *55* (1), 164–174.

(20) Zhang, B.; Wang, X.; Zhu, A.; Ma, K.; Lv, Y.; Wang, X.; An, Z. Enzyme-Initiated Reversible Addition–Fragmentation Chain Transfer Polymerization. *Macromolecules* **2015**, *48* (21), 7792–7802.

(21) Chapman, R.; Gormley, A. J.; Stenzel, M. H.; Stevens, M. M. Combinatorial Low-Volume Synthesis of Well-Defined Polymers by Enzyme Degassing. *Angew. Chemie Int. Ed.* **2016**, *55* (14), 4500–4503.

(22) Chapman, R.; Gormley, A. J.; Herpoldt, K.-L.; Stevens, M. M. Highly Controlled Open Vessel RAFT Polymerizations by Enzyme Degassing. *Macromolecules* **2014**, *47* (24), 8541–8547.

(23) Corrigan, N.; Zhernakov, L.; Hashim, M. H.; Xu, J.; Boyer, C. Flow Mediated Metal-Free PET-RAFT Polymerisation for Upscaled and Consistent Polymer Production. *React. Chem. Eng.* **2019**, *4* (7), 1216–1228.

(24) Zavada, S. R.; Battsengel, T.; Scott, T. F. Radical-Mediated Enzymatic Polymerizations. *Int. J. Mol. Sci.* **2016**, *17* (2).

(25) Zhao, B.; Li, J.; Xiu, Y.; Pan, X.; Zhang, Z.; Zhu, J. Xanthate-Based Photoiniferter RAFT Polymerization toward Oxygen-Tolerant and Rapid Living 3D Printing. *Macromolecules* **2022**, *55* (5), 1620–1628.

(26) Lu, L.; Zhang, H.; Yang, N.; Cai, Y. Toward Rapid and Well-Controlled Ambient Temperature RAFT Polymerization under UV−Vis Radiation: Effect of Radiation Wave Range. *Macromolecules* **2006**, *39* (11), 3770–3776.

(27) Fu, Q.; Xie, K.; McKenzie, T. G.; Qiao, G. G. Trithiocarbonates as Intrinsic Photoredox Catalysts and RAFT Agents for Oxygen Tolerant Controlled Radical Polymerization. *Polym. Chem.* **2017**, *8* (9), 1519–1526.

(28) Quinn, J. F.; Barner, L.; Barner-Kowollik, C.; Rizzardo, E.; Davis, T. P. Reversible Addition−Fragmentation Chain Transfer Polymerization Initiated with Ultraviolet Radiation. *Macromolecules* **2002**, *35* (20), 7620–7627.

(29) McKenzie, T. G.; Fu, Q.; Wong, E. H. H.; Dunstan, D. E.; Qiao, G. G. Visible Light Mediated Controlled Radical Polymerization in the Absence of Exogenous Radical Sources or Catalysts. *Macromolecules* **2015**, *48* (12), 3864–3872.

(30) Wang, J.; Rivero, M.; Muñoz Bonilla, A.; Sanchez-Marcos, J.; Xue, W.; Chen, G.; Zhang, W.; Zhu, X. Natural RAFT Polymerization: Recyclable-Catalyst-Aided, Opened-to-Air, and Sunlight-Photolyzed RAFT Polymerizations. *ACS Macro Lett.* **2016**, *5* (11).

(31) Bagheri, A.; Engel, K. E.; Bainbridge, C. W. A.; Xu, J.; Boyer, C.; Jin, J. 3D Printing of Polymeric Materials Based on Photo-RAFT Polymerization. *Polym. Chem.* **2020**, *11* (3), 641–647.

(32) Lamb, J. R.; Qin, K. P.; Johnson, J. A. Visible-Light-Mediated, Additive-Free, and Open-to-Air Controlled Radical Polymerization of Acrylates and Acrylamides. *Polym. Chem.* **2019**, *10* (13), 1585–1590.

(33) Nothling, M. D.; Fu, Q.; Reyhani, A.; Allison-Logan, S.; Jung, K.; Zhu, J.; Kamigaito, M.; Boyer, C.; Qiao, G. G. Progress and Perspectives Beyond Traditional RAFT Polymerization. *Adv. Sci.* **2020**, *7* (20), 2001656.

(34) Calitz, F. M.; Tonge, M. P.; Sanderson, R. D. Kinetic and Electron Spin Resonance Analysis of RAFT Polymerization of Styrene. *Macromolecules*. 2003, pp 5–8.

(35) Tanaka, J.; Gurnani, P.; Cook, A. B.; Häkkinen, S.; Zhang, J.; Yang, J.; Kerr, A.; Haddleton, D. M.; Perrier, S.; Wilson, P. Microscale Synthesis of Multiblock Copolymers Using Ultrafast RAFT Polymerisation. *Polym. Chem.* **2019**, *10* (10), 1186–1191.

(36) Kuroki, A.; Martinez-Botella, I.; Hornung, C. H.; Martin, L.; Williams, E. G. L.; Locock, K. E. S.; Hartlieb, M.; Perrier, S. Looped Flow RAFT Polymerization for Multiblock Copolymer Synthesis. *Polym. Chem.* **2017**, *8* (21), 3249–3254.

(37) Gody, G.; Barbey, R.; Danial, M.; Perrier, S. Ultrafast RAFT Polymerization: Multiblock Copolymers within Minutes. *Polym. Chem.* **2015**, *6* (9), 1502–1511.

(38) Cosson, S.; Danial, M.; Saint-Amans, J. R.; Cooper-White, J. J. Accelerated Combinatorial High

Throughput Star Polymer Synthesis via a Rapid One-Pot Sequential Aqueous RAFT (Rosa-RAFT) Polymerization Scheme. *Macromol. Rapid Commun.* **2017**, *38* (8), 1600780.

(39) Parkinson, S.; Knox, S. T.; Bourne, R. A.; Warren, N. J. Rapid Production of Block Copolymer Nano-Objects via Continuous-Flow Ultrafast RAFT Dispersion Polymerisation. *Polym. Chem.* **2020**, *11* (20), 3465–3474.

(40) Gurnani, P.; Floyd, T.; Tanaka, J.; Stubbs, C.; Lester, D.; Sanchez-Cano, C.; Perrier, S. PCR-RAFT: Rapid High Throughput Oxygen Tolerant RAFT Polymer Synthesis in a Biology Laboratory. *Polym. Chem.* **2020**, *11* (6), 1230–1236.

(41) Reis, M.; Gusev, F.; Taylor, N. G.; Chung, S. H.; Verber, M. D.; Lee, Y. Z.; Isayev, O.; Leibfarth, F. A. Machine-Learning-Guided Discovery of 19 F MRI Agents Enabled by Automated Copolymer Synthesis. *J. Am. Chem. Soc.* **2021**, *143* (42), 17677–17689.

(42) Rubens, M.; Vrijsen, J. H.; Laun, J.; Junkers, T. Precise Polymer Synthesis by Autonomous Self-Optimizing Flow Reactors. *Angew. Chemie* **2019**, *131* (10), 3215–3219.

(43) Reis, M. H.; Varner, T. P.; Leibfarth, F. A. The Influence of Residence Time Distribution on Continuous-Flow Polymerization. *Macromolecules* **2019**, *52* (9), 3551–3557.

(44) Walsh, D. J.; Schinski, D. A.; Schneider, R. A.; Guironnet, D. General Route to Design Polymer Molecular Weight Distributions through Flow Chemistry. *Nat. Commun.* **2020**, *11* (1).

(45) Reis, M. H.; Davidson, C. L. G.; Leibfarth, F. A. Continuous-Flow Chemistry for the Determination of Comonomer Reactivity Ratios. *Polym. Chem.* **2018**, *9* (13), 1728–1734.

(46) Reis, M. H.; Leibfarth, F. A.; Pitet, L. M. Polymerizations in Continuous Flow: Recent Advances in the Synthesis of Diverse Polymeric Materials. *ACS Macro Lett.* **2020**, *9* (1), 123–133.

(47) Sato, T.; Hamada, Y.; Sumikawa, M.; Araki, S.; Yamamoto, H. Solubility of Oxygen in Organic Solvents and Calculation of the Hansen Solubility Parameters of Oxygen. *Ind. Eng. Chem. Res.* **2014**, *53* (49), 19331–19337.

(48) Robischon, M. Surface-Area-to-Volume Ratios, Fluid Dynamics & Gas Diffusion: Four Frogs & Their Oxygen Flux. *Am. Biol. Teach.* **2017**, *79* (1), 64–67.

(49) Kucernak, A.; Jiang, J. Mesoporous Platinum as a Catalyst for Oxygen Electroreduction and Methanol Electrooxidation. *Chem. Eng. J.* **2003**, *93* (1), 81–90.

(50) Vandegriff, K. D.; Olson, J. S. Morphological and Physiological Factors Affecting Oxygen Uptake and Release by Red Blood Cells. *J. Biol. Chem.* **1984**, *259* (20), 12619–12627.

(51) Flores-López, L. Z.; Espinoza-Gómez, H.; Somanathan, R. Silver Nanoparticles: Electron Transfer, Reactive Oxygen Species, Oxidative Stress, Beneficial and Toxicological Effects. Mini Review. *J. Appl. Toxicol.* **2019**, *39* (1), 16–26.

(52) Mair, R. W.; Wong, G. P.; Hoffmann, D.; Hürlimann, M. D.; Patz, S.; Schwartz, L. M.; Walsworth, R. L. Probing Porous Media with Gas Diffusion NMR. *Phys. Rev. Lett.* **1999**, *83* (16), 3324–3327.

(53) Wilken, S.; Parisi, J.; Borchert, H. Role of Oxygen Adsorption in Nanocrystalline ZnO Interfacial Layers for Polymer–Fullerene Bulk Heterojunction Solar Cells. *J. Phys. Chem. C* **2014**, *118* (34),

19672–19682.

(54) Gershon, N. D.; Porter, K. R.; Trus, B. L. The Cytoplasmic Matrix: Its Volume and Surface Area and the Diffusion of Molecules through It. *Proc. Natl. Acad. Sci.* **1985**, *82* (15), 5030–5034.

(55) Shanmugam, S.; Xu, J.; Boyer, C. Utilizing the Electron Transfer Mechanism of Chlorophyll a under Light for Controlled Radical Polymerization. *Chem. Sci.* **2015**, *6* (2), 1341–1349.

(56) Shanmugam, S.; Xu, J.; Boyer, C. Photoinduced Electron Transfer–Reversible Addition–Fragmentation Chain Transfer (PET-RAFT) Polymerization of Vinyl Acetate and N - Vinylpyrrolidinone: Kinetic and Oxygen Tolerance Study. *Macromolecules* **2014**, *47* (15), 4930–4942.

(57) Shanmugam, S.; Xu, J.; Boyer, C. Aqueous RAFT Photopolymerization with Oxygen Tolerance. *Macromolecules* **2016**, *49* (24), 9345–9357.

(58) Shen, L.; Lu, Q.; Zhu, A.; Lv, X.; An, Z. Photocontrolled RAFT Polymerization Mediated by a Supramolecular Catalyst. *ACS Macro Lett.* **2017**, *6* (6), 625–631.

(59) Xu, J.; Shanmugam, S.; Fu, C.; Aguey-Zinsou, K.-F.; Boyer, C. Selective Photoactivation: From a Single Unit Monomer Insertion Reaction to Controlled Polymer Architectures. *J. Am. Chem. Soc.* **2016**, *138* (9), 3094–3106.

(60) Song, Y.; Kim, Y.; Noh, Y.; Singh, V. K.; Behera, S. K.; Abudulimu, A.; Chung, K.; Wannemacher, R.; Gierschner, J.; Lüer, L.; et al. Organic Photocatalyst for Ppm-Level Visible-Light-Driven Reversible Addition–Fragmentation Chain-Transfer (RAFT) Polymerization with Excellent Oxygen Tolerance. *Macromolecules* **2019**, *52* (15), 5538–5545.

(61) Niu, J.; Page, Z. A.; Dolinski, N. D.; Anastasaki, A.; Hsueh, A. T.; Soh, H. T.; Hawker, C. J. Rapid Visible Light-Mediated Controlled Aqueous Polymerization with In Situ Monitoring. *ACS Macro Lett.* **2017**, *6* (10), 1109–1113.

(62) Xu, J.; Jung, K.; Boyer, C. Oxygen Tolerance Study of Photoinduced Electron Transfer–Reversible Addition–Fragmentation Chain Transfer (PET-RAFT) Polymerization Mediated by Ru(Bpy) 3 Cl 2. *Macromolecules* **2014**, *47* (13), 4217–4229.

(63) Shanmugam, S.; Xu, J.; Boyer, C. Exploiting Metalloporphyrins for Selective Living Radical Polymerization Tunable over Visible Wavelengths. *J. Am. Chem. Soc.* **2015**, *137* (28), 9174–9185.

(64) Benaglia, M.; Chiefari, J.; Chong, Y. K.; Moad, G.; Rizzardo, E.; Thang, S. H. Universal (Switchable) RAFT Agents. *J. Am. Chem. Soc.* **2009**, *131* (20).

(65) Mukundan, T.; Kishore, K. Synthesis, Characterization and Reactivity of Polymeric Peroxides. *Prog. Polym. Sci.* **1990**, *15* (3), 475–505.

(66) Zhang, Z.; Zhu, J.; Cheng, Z.; Zhu, X. Reversible Addition–Fragmentation Chain Transfer (RAFT) Polymerization of Styrene in the Presence of Oxygen. *Polymer (Guildf).* **2007**, *48* (15), 4393–4400.

(67) Cais, R. E.; Bovey, F. A. Carbon-13 Nuclear Magnetic Resonance Study of the Microstructure and Molecular Dynamics of Poly(Styrene Peroxide). *Macromolecules* **1977**, *10* (1), 169–178.

(68) Kishore, K. Spectral and Thermal Data on Polystyrene Peroxide. *J. Chem. Eng. Data* **1980**, *25* (1),

92–94.

(69) Jayanthi, S.; Kishore, K. Oxidative Copolymerization: Microstructure Analysis of the Terpolymer of Styrene, Methyl Methacrylate, and Oxygen. *Macromolecules* **1993**, *26* (8), 1985–1989.

(70) L. Villaraza, A. J.; Bumb, A.; Brechbiel, M. W. Macromolecules, Dendrimers, and Nanomaterials in Magnetic Resonance Imaging: The Interplay between Size, Function, and Pharmacokinetics. *Chem. Rev.* **2010**, *110* (5), 2921–2959.

(71) Zaquen, N.; Rubens, M.; Corrigan, N.; Xu, J.; Zetterlund, P. B.; Boyer, C.; Junkers, T. Polymer Synthesis in Continuous Flow Reactors. *Prog. Polym. Sci.* **2020**, *107*, 101256.

(72) Moore, J. S.; Jensen, K. F. "Batch" Kinetics in Flow: Online IR Analysis and Continuous Control. *Angew. Chemie Int. Ed.* **2014**, *53* (2), 470–473.